Journal of Materials Chemistry A

ROYAL SOCIETY OF CHEMISTRY

PAPER

View Article Online
View Journal | View Issue

Cite this: J. Mater. Chem. A, 2022, 10, 18156

Improving hydrogen production for carbon-nitride-based materials: crystallinity, cyanimide groups and alkali metals in solution working synergistically†

Ivo F. Teixeira, *[ab] Nadezda V. Tarakina, [b] Ingrid F. Silva, [bc] Gabriel Ali Atta Diab, [a] Nieves López Salas, [b] Aleksandr Savateev [b] and Markus Antonietti [b]

Received 13th July 2022
Accepted 13th August 2022

DOI: 10.1039/d2ta05571f

rsc.li/materials-a

The recent findings on the fundamental understanding of the activity of carbon nitride-based materials in the hydrogen evolution reaction (HER) allow to design rationally the photocatalytic systems with improved activities. Herein, combining highly ordered materials with cyanimide defects and alkali metal cations in the solution, we demonstrated an important synergistic effect which for cyanimide modified K-PHI is revealed in 12 times higher apparent quantum yield (AQY) compared to K-PHI free of surface cyanimide groups.

Introduction

Providing energy in a sustainable manner to power future development of humankind will necessarily require key green technologies, such as the synthesis of renewable fuels. Hydrogen is one of the promising candidates to become a renewable energy carrier in the future and it will be an essential reactant to enable a sustainable route to CO_2 reduction. However, storage of hydrogen gas is very challenging. Consequently, its use to reduce CO_2 to liquid fuels *e.g.* methanol and higher alcohols is more promising.[1,2] Nevertheless, it is important to emphasize that nowadays 96% of commercial hydrogen is generated from fossil fuels.[3] Therefore, using non-fossil hydrogen sources is essential to make CO_2 reduction technology sustainable. Amongst the methods available to generate hydrogen gas, undoubtedly, water splitting photocatalyzed by semiconductors under sunlight stands out.[4]

In the last two decades, carbon nitride-based materials have been widely tested in hydrogen evolution from water under different conditions. Often hole or electron scavengers are added to remove one of the photogenerated charge carrier efficiently from the photocatalyst and only half-reaction is investigated.[5] Although polymeric carbon nitride (PCN) stands out as the most investigated carbon nitride-based material in the hydrogen evolution reaction (HER), pristine PCN displays a poor activity even in the presence of scavengers.[6–12] However, the recently developed carbon nitride materials synthesized in the presence of an inorganic salt, such as NaCl,[13] KCl and LiCl, give highly crystalline photocatalysts with enhanced efficiency in the HER.[14–20]

As illustrated in Fig. 1, a successful HER depends on four consecutive processes: (1) photon absorption; (2) charge

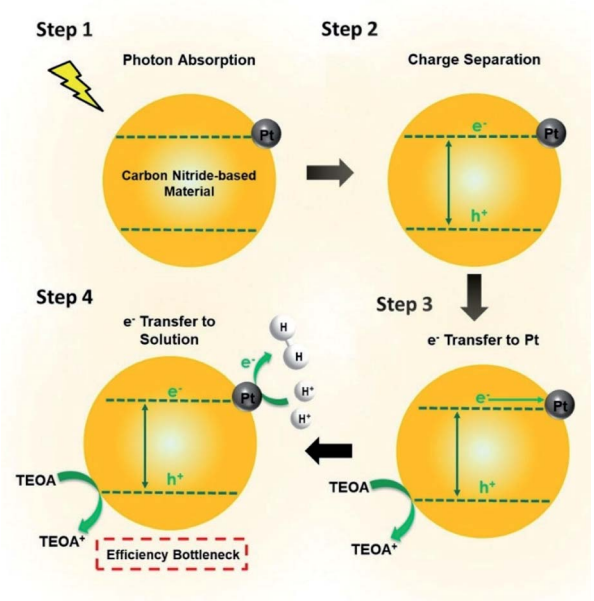

Fig. 1 Schematic representation of steps involved in the HER: (1) photon absorption; (2) charge separation; (3) e^- transfer to Pt NPs and (4) e^- transfer to solution.

[a]Department of Chemistry, Federal University of São Carlos, 13565-905, São Carlos, SP, Brazil. E-mail: ivo@ufscar.br

[b]Department of Colloid Chemistry, Max Planck Institute of Colloids and Interfaces, Am Mühlenberg 1, D-14476 Potsdam, Germany. E-mail: Markus.Antonietti@mpikg.mpg.de

[c]Department of Chemistry, ICEx, Federal University of Minas Gerais, 31270-901, Belo Horizonte, MG, Brazil

† Electronic supplementary information (ESI) available. See https://doi.org/10.1039/d2ta05571f

separation; (3) transfer of photogenerated electron to the co-catalyst (Pt), and (4) electron transfer from the co-catalyst to the solution-based reactant. The last step is particularly important for highly optimized systems, such as ordered carbon nitride materials, as we demonstrated in a recent work.[21] However, when the electron transfer in the step 4 is optimized, for example, by adding alkali metals to the solution, it is possible to further improve the system by tuning other reaction steps. As the efficiency of the overall electron transfer process is also dependent on the effective transfer of the electron to the co-catalyst in step 3 (here Pt), applying strategies to promote this transfer together with the alkali metal salts added to the solution might lead to a synergistic effect and even higher activities. The same approach can be employed in the charge separation step 2.

In a recent work, we verified that the electron transfer from Pt NP to the solution in step 4 was the bottleneck step for highly ordered carbon nitride-based materials, *i.e.* sodium and potassium poly(heptazine imide)s, Na-PHI and K-PHI, respectively.[21] Once the bottleneck was eliminated by the addition of alkali metal salts to the reaction mixture solution a new horizon has opened for further optimization of the HER.

Herein we systematically investigate performance of a series of carbon nitride-based material in the HER with and without alkali metal salts added to the solution. We observe a synergistic effect between highly ordered structures, cyanimide groups grafted to the surface of the photocatalysts and presence of alkali metals ions in the solution. In will be shown here that this optimization allows for an another 12-fold increase of the AQY for cyanimide modified K-PHI.

Results and discussion

Characterization of carbon nitride-based materials

A series of carbon nitride-based materials were synthesized. The chemical composition for the synthesized materials were determined by elemental analysis, inductively coupled plasma optical emission spectrometry (ICP-OES) and thermogravimetric analysis, the results are presented in Table S1 in the ESI.† High-resolution transmission electron microscopy (HR-TEM) images and the corresponding Fast Fourier transforms (FFT) confirm formation of crystalline materials (Fig. 2). FFTs were indexed in hexagonal symmetry, however small distortions from ideal hexagonal symmetry have been found in most of the samples. CN-OA-m displays much smaller grains with different degree of crystallinity, which tend to form agglomerates. LiK-PHI also showed more defect structure, which can be clearly seen from FFTs and corresponding XRD pattern. Na-PHI and K-PHI-based materials were found to form big flakes consisting of crystalline domains of about 100 nm in size.

As shown in Fig. 3a, all the samples display intense peaks at around 8 and 27°. The former corresponds to the (1−10) planes in the crystal representing periodicity in between the heptazine columns and the latter corresponds to the (001) planes showing interplanar stacking.[22,23] The Fourier-transform infrared (FTIR) spectra for all the carbon nitride-based materials are fairly similar (Fig. 3b). All the samples display bands typical for heptazine-based carbon nitrides, *i.e.* 1107, 985 and 796 cm^{-1}.[24,25] It is also worth noting that the band at 1206 cm^{-1} is related to aromatic amine C–N stretching[24,25] as well as the band at 2179 cm^{-1} is related to the vibration of cyanamide groups.[26]

The bandgaps of the samples presented in Fig. 3d were determined from the UV-Vis diffuse reflectance absorption spectra (DRS) by applying the method reported by Makuła *et al.*[27] (Fig. 3c). The obtained band gaps range from 2.32 eV for CN-OA-m up to 2.78 eV for Na-PHI and NCN-K-PHI, which are not very different compared to PCN (2.7 eV)[28,29] and other heptazine–based materials. Bands positions (Fig. 3d) were estimated by adding band gap values to the flat band potentials obtained from the Mott–Schottky plots (Fig. S3 and Table S2†). The sample NCN-K-PHI displays the most oxidative valence band (2.62 V *vs.* NHE), while K-PHI presented the most

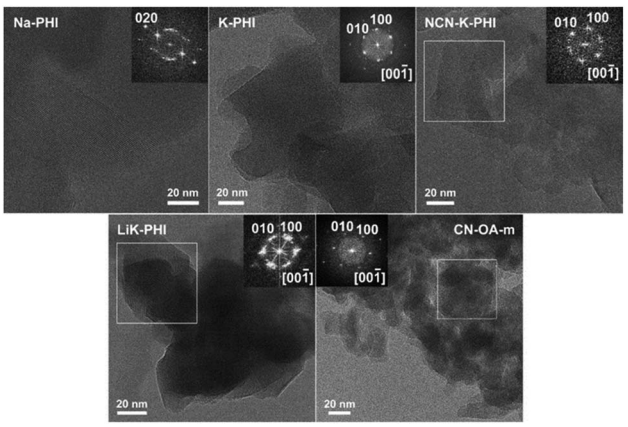

Fig. 2 HR-TEM images of carbon nitride-based samples, with FFT shown in the insets. FFTs are taken from the complete image unless indicated by white squares.

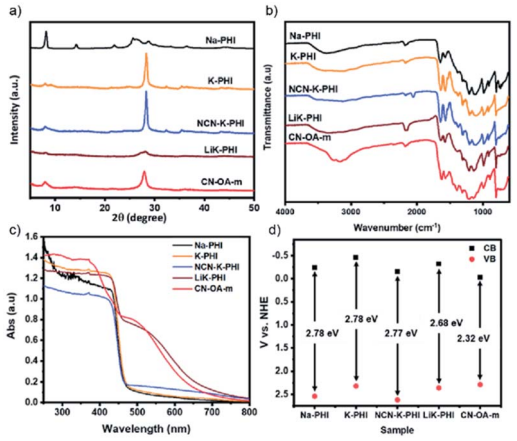

Fig. 3 (a) Powder XRD patterns; (b) FT-IR spectra; (c) UV-Vis diffuse reflectance absorption spectra (DRS); (d) estimated band positions of all tested carbon nitride-based materials (*i.e.* Na-PHI, K-PHI, NCN-K-PHI, LiK-PHI and CN-OA-m).

reductive conduction band (−0.46 V *vs.* NHE). As previously reported by Zhang *et al.* the samples CN-OA-m and LiK-PHI display a broader absorption in the visible range (Fig. 3c), due to intraband states in their electronic structure.[30,31]

The samples were also characterized by X-ray photoelectron spectroscopy (XPS). As shown in Fig. 4, the C1s signal for the Na-PHI sample can be deconvoluted into three peaks, with the binding energies at 288.2, 286.8 and 284.8 eV, to be assigned to CN_3 (carbon in the heterocycle ring), surficial C-OH and adventitious carbon, respectively. The N1s for the same sample displays peaks assigned to NC_3 in the center of the heptazine rings (401.1 eV), NC_2 atoms in the heptazine ring (398.7 eV), and partially negative nitrogen atoms connecting two heptazine rings (396.7 eV).[32,33] LiK-PHI, K-PHI and NCN-K-PHI samples display the same set of peaks, however, K2s peaks can be noticed in the C1s spectra and one peak at higher binding energy is present for N1s spectra for LiK-PHI, which is attributed to N–O (403 eV).[34] The sample CN-OA-m displays essentially the same peaks with potassium peaks less intense compared to the other potassium samples, which is in agreement with the ICP results (Table S1†). In the N1s spectra, this sample does not present peaks related to NC_2 atoms in the heptazine ring at 396.7 eV, which indicates that this nitrogen might be functionalized or oxidized shifting its binding energy to 404.3 eV (N–O).[31]

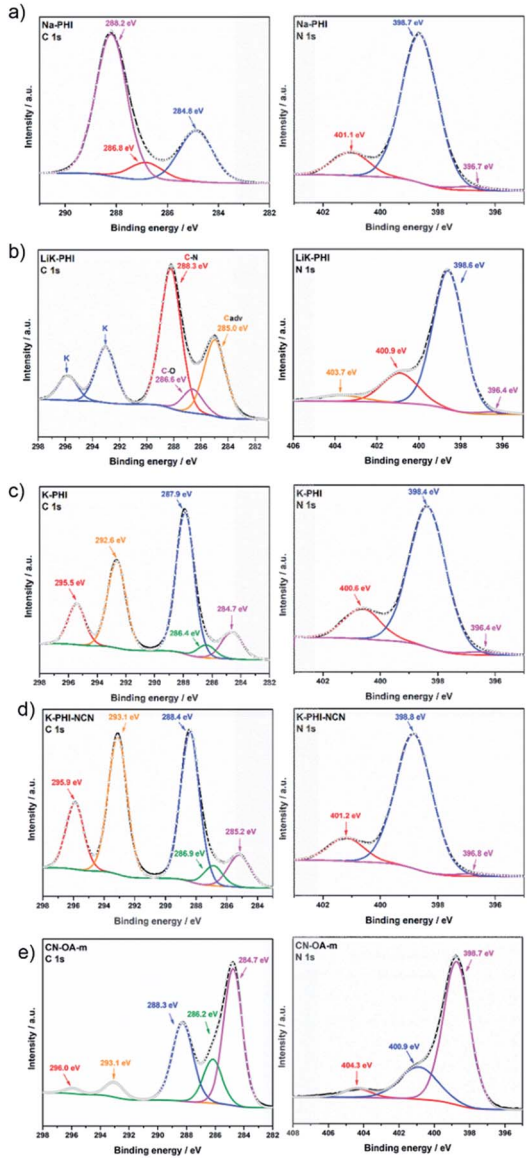

Fig. 4 C1s and N1s for (a) Na-PHI; (b) LiK-PHI; (c) K-PHI; (d) NCN-K-PHI and (e) CN-OA-m.

Photocatalytic tests

The synthesized carbon nitride-based materials were tested in H_2 evolution. The results are summarized in Fig. 5. By adding LiCl (1 mol L^{-1}) all the samples displayed an increment in the H_2 evolution rate (Fig. 5), confirming that the effect of added alkali metal cations previously demonstrated by our group for Na-PHI is effective for a broader range of carbon nitride materials (Fig. 5a and b).[21] Despite all carbon nitride materials display an increased activity when alkali salts are added to the aqueous solution, these increases occur along different orders of magnitude. For example, addition of LiCl to the reaction mixture containing materials with higher crystallinity (Na-PHI, K-PHI and NCN-K-PHI) drastically enhances the activity. These results can be explained by more facile electron transfer from the semiconductor to the co-catalyst. However, the electron transfer depends not only on the mobility of charge carriers, which in turn is facilitated by highly ordered structures, but also on the interface between the carbon nitride material and the co-catalyst.[4,21,35]

The presence of cyanamide groups provides a collaborative effect inducing an internal electrical field improving the separation of photoexcited charge carriers and inhibiting their recombination, as shown in the Fig. 5c by the shorter $\tau_{0.5}$ time for the cyanimide treated K-PHI sample (NCN-K-PHI).[36] In addition, as demonstrated by Lotsch *et al.*, cyanamide-defects enhance co-catalyst interaction and facilitates the electron transfer to the metal sites. The functionalization of polymeric carbon nitride (PCN) with extra cyanamide groups, leads to 12 to 16-fold more active photocatalysts in the HER.[37] The participation of the cyanimide groups can be confirmed by comparing the activity of K-PHI with the NCN-K-PHI (material obtained after treatment of K-PHI with KSCN). This treatment is a standard method to improve the number of cyanimide defects on the surface of the material. After the treatment, the K-PHI activity for the sample increases with and without the presence of LiCl. However, this increment is significantly more important in the presence of LiCl (Fig. 5b), where the NCN-K-PHI displays a AQY of 12%, indicating a synergistic effect between the surface-cyanimide groups and the alkali metal in solution.

As shown in Fig. 5b, the remarkable increments of the AQY (measured at 420 nm) are all observed for the samples in the presence of LiCl. However, it is worth highlighting that NCN-K-PHI displays a 12-fold boost in AQY, the highest gain among all the tested samples. This increment can be attributed to a highly crystalline structure, in case of Na-PHI and K-PHI, along with an

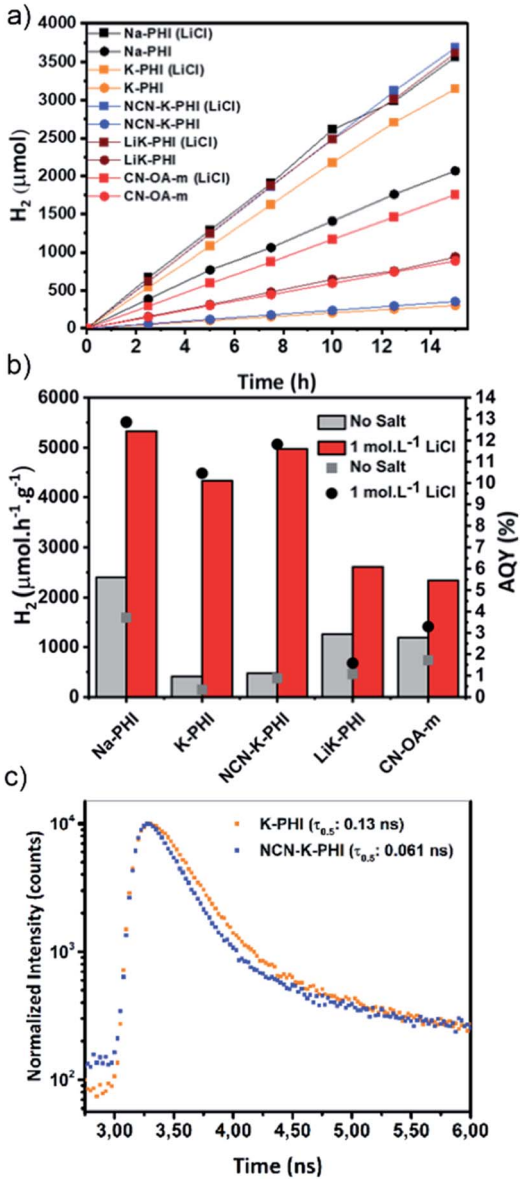

Fig. 5 (a) Time course of the HER acquired using 50 mg of carbon nitride-based material with and without LiCl in solution (1.0 mol L^{-1}); (b) H_2 evolution rate for different carbon nitride-based materials with 1 mol L^{-1} of LiCl (red) and without (gray) at 410 nm irradiation. The AQY (at 420 nm) for the carbon nitride-based materials obtained with 1 mol L^{-1} of LiCl added to the reaction mixture (black circles) and without (gray squares) is reported at the right axis; (c) Time-resolved photoluminescence of K-PHI and the same sample treated with KSCN with respective radiative lifetimes ($\tau_{0,5}$).

improved electron transfer to the Pt co-catalyst due to the presence of cyanimide groups (Fig. 7). Furthermore, as evidenced by the Tr-PL analysis (Fig. 5c) the cyanimide groups also display an important promoting effect in the charge separation process, due to the internal electrical field promoted by the cyanimide defects.[36] As in the presence of alkali metal cations, the electron transfer from the Pt to the solution is no longer the rate limiting step, the previous steps (*i.e.* charge separation and electron transfer from the carbon nitride to the co-catalyst) becomes the bottleneck for the HER.

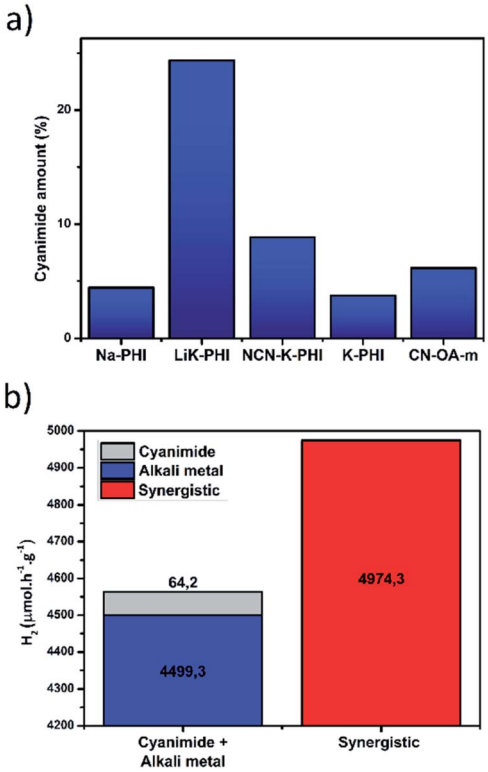

Fig. 6 (a) Relative amount of cyanimide in the structure of such catalyst, estimated using FT-IR data, integrating the signal associated with the cyanimide groups standardized by the bands in the range between 1500 and 1700 cm^{-1} corresponding to heptazines stretching. (b) Graphical illustration demonstrating the synergistic effect when each strategy is employed simultaneously compared to the sum of each contribution in the situation that are used separately. Data calculated comparing K-PHI and NCN-K-PHI.

An analysis of the relative amount of cyanimide defects in the structure (Fig. 6a) shows that the LiK-PHI catalyst contains defects in greater density in the structure, however it shows low activity, even in the presence of alkali salt. This agrees with its low crystallinity as demonstrated by XRD patterns. In contrast, crystalline materials as Na-PHI, NCN-K-PHI and K-PHI balance all strategies resulting in higher activity, reinforcing that there

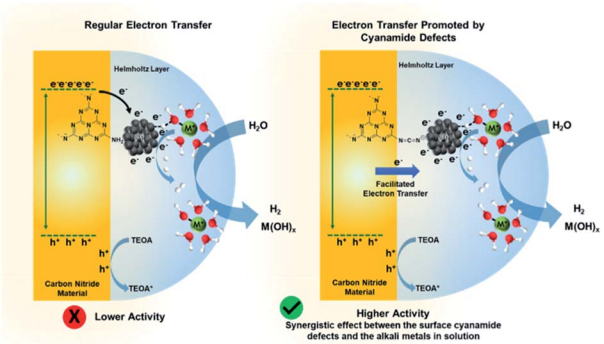

Fig. 7 Schematic comparison of the HER photocatalysed by carbon nitride-based materials with and without cyanamide defects.

is a collaborative effect between crystallinity, cyano defects and alkali salt presence.

Comparing the hydrogen evolution rate of K-PHI and NCN-K-PHI, there is an improvement of 64.2 μmol h^{-1} g^{-1} in absence of alkali salt, thus it can be associated to the cyanimide contribution (Fig. 6b). Comparing the HER of NCN-K-PHI in presence/absence of alkali metal, it is noticed a 4499.3 μmol h^{-1} g^{-1} increment, which can be associated solely to alkali salt contribution. In opposition, when both strategies are used simultaneously, the HER increase to 4974.3 μmol h^{-1} g^{-1} which is superior in 410.8 μmol h^{-1} g^{-1} the sum of both strategies used separately (Fig. 6b). In this way, there is not a sum of positive effects, but contributions working synergistically (Fig. 7).

Recyclability tests were performed for the most active sample, *i.e.* Na-PHI. The sample was tested in 4 independent and consecutive cycles, which consisted in run the reaction, recovering the sample by centrifugation after a 24 h reaction, washing the sample with water, drying overnight and running a new cycle. After 4 cycles the activity is preserved, as shown in Fig. S2.†

Conclusions

In summary, we have demonstrated that by combining highly ordered carbon nitride materials, cyanimide defects and alkali metal ions in solution an important synergistic effect arises. This effect allows pushing further the activities and AQY for a range of ordered carbon nitride materials. The sample NCN-K-PHI possessing surface cyanimide defects and prepared by treatment of K-PHI with KSCN, displays a 12-fold increment in its activity. These findings are important for rational design of highly active carbon nitride materials and construction of the photocatalytic systems with higher H_2 evolution rates and AQY.

Author contributions

IFT conceived and coordinated all stages of this research in collaboration with MA. IFT prepared the catalyst. IFT, NDT and IFS characterized the catalysts. IFT and IFS undertook the HER tests. NDT conducted the AC-STEM analysis. IFS collected the Tr-PL and GAAD interpreted and discussed it. IFT, AS, MA, NDT, GAAD and IFS co-wrote the manuscript in discussion with other co-authors.

Conflicts of interest

The authors declare no competing financial interest.

Acknowledgements

This research was supported financially by the Max Planck Society. The authors IFT and IFS are grateful to the Brazilian funding agencies CAPES, CNPq (423196/2018-9 and 403064/2021-0) and FAPESP (2020/14741-6, 2021/13915-3 and 2021/11162-8) for financial support. I. F. T. thanks the Alexander von Humboldt Foundation for his postdoctoral fellowship. Dr Johannes Schmidt is greatly acknowledged for his support with XPS analysis. Tobias Heil, Bolortuya Badamdorj and Diana Piankova are greatly acknowledged for their support with TEM data collection. Open Access funding provided by the Max Planck Society.

References

1 M. M. J. Li, C. Chen, T. Ayvalı, H. Suo, J. Zheng, I. F. Teixeira, L. Ye, H. Zou, D. O'Hare and S. C. E. Tsang, *ACS Catal.*, 2018, **8**, 4390–4401.
2 C. H. Vo, C. Mondelli, H. Hamedi, J. Pérez-Ramírez, S. Farooq and I. A. Karimi, *ACS Sustainable Chem. Eng.*, 2021, **9**, 10591–10600.
3 P. Nikolaidis and A. Poullikkas, *Renew. Sustain. Energy Rev.*, 2017, **67**, 597–611.
4 L. Lin, Z. Lin, J. Zhang, X. Cai, W. Lin, Z. Yu and X. Wang, *Nat. Catal.*, 2020, **3**, 649–655.
5 W. Yang, R. Godin, H. Kasap, B. Moss, Y. Dong, S. A. J. Hillman, L. Steier, E. Reisner and J. R. Durrant, *J. Am. Chem. Soc.*, 2019, **141**, 11219–11229.
6 M. Zhang, X. Bai, D. Liu, J. Wang and Y. Zhu, *Appl. Catal. B Environ.*, 2015, **164**, 77–81.
7 Q. Lin, L. Li, S. Liang, M. Liu, J. Bi and L. Wu, *Appl. Catal. B Environ.*, 2015, **163**, 135–142.
8 Y. Di, X. Wang, A. Thomas and M. Antonietti, *ChemCatChem*, 2010, **2**, 834–838.
9 Y. Zheng, L. Lin, B. Wang and X. Wang, *Angew. Chem., Int. Ed.*, 2015, **54**, 12868–12884.
10 Y. Zheng, L. Lin, B. Wang and X. Wang, *Angew. Chem.*, 2015, **127**, 13060–13077.
11 F. K. Kessler, Y. Zheng, D. Schwarz, C. Merschjann, W. Schnick, X. Wang and M. J. Bojdys, *Nat. Rev. Mater.*, 2017, **2**, 1–17.
12 W.-J. Ong, L.-L. Tan, Y. H. Ng, S.-T. Yong and S.-P. Chai, *Chem. Rev.*, 2016, **116**, 7159–7329.
13 M. A. R. da Silva, I. F. Silva, Q. Xue, B. T. W. Lo, N. V. Tarakina, B. N. Nunes, P. Adler, S. K. Sahoo, D. W. Bahnemann, N. López-Salas, A. Savateev, C. Ribeiro, T. D. Kühne, M. Antonietti and I. F. Teixeira, *Appl. Catal. B Environ.*, 2022, **304**, 120965.
14 G. Zhang, Y. Xu, D. Yan, C. He, Y. Li, X. Ren, P. Zhang and H. Mi, *ACS Catal.*, 2021, **11**, 6995–7005.
15 G. Zhang, Y. Xu, C. He, P. Zhang and H. Mi, *Appl. Catal. B Environ.*, 2021, **283**, 119636.
16 S. K. Sahoo, I. F. Teixeira, A. Naik, J. Heske, D. Cruz, M. Antonietti, A. Savateev and T. D. Kühne, *J. Phys. Chem. C*, 2021, **125**, 13749–13758.
17 W. Iqbal, B. Qiu, Q. Zhu, M. Xing and J. Zhang, *Appl. Catal. B Environ.*, 2018, **232**, 306–313.
18 W.-C. Lin, S. Wu, G. Li, P.-L. Ho, Y. Ye, P. Zhao, S. Day, C. Tang, W. Chen and A. Zheng, *Chem. Sci.*, 2020, **12**, 210–219.
19 G. Algara-Siller, N. Severin, S. Y. Chong, T. Björkman, R. G. Palgrave, A. Laybourn, M. Antonietti, Y. Z. Khimyak, A. V. Krasheninnikov and J. P. Rabe, *Angew. Chem., Int. Ed.*, 2014, **53**, 7450–7455.

20 L. Lin, C. Wang, W. Ren, H. Ou, Y. Zhang and X. Wang, *Chem. Sci.*, 2017, **8**, 5506–5511.
21 I. F. Teixeira, N. V. Tarakina, I. F. Silva, N. López-Salas, A. Savateev and M. Antonietti, *Adv. Sustain. Syst.*, 2022, 2100429.
22 A. Savateev, S. Pronkin, M. G. Willinger, M. Antonietti and D. Dontsova, *Chem.–Asian J.*, 2017, **12**, 1517–1522.
23 F. M. Colombari, M. A. R. da Silva, M. S. Homsi, B. R. L. de Souza, M. Araujo, J. L. Francisco, G. T. S. T. da Silva, I. F. Silva, A. F. de Moura and I. F. Teixeira, *Faraday Discuss.*, 2021, **227**, 306–320.
24 B. V. Lotsch and W. Schnick, *Chem. Mater.*, 2006, **18**, 1891–1900.
25 D. Dontsova, S. Pronkin, M. Wehle, Z. Chen, C. Fettkenhauer, G. Clavel and M. Antonietti, *Chem. Mater.*, 2015, **27**, 5170–5179.
26 V. W.-h. Lau, I. Moudrakovski, T. Botari, S. Weinberger, M. B. Mesch, V. Duppel, J. Senker, V. Blum and B. V. Lotsch, *Nat. Commun.*, 2016, **7**, 12165.
27 P. Makuła, M. Pacia and W. Macyk, *J. Phys. Chem. Lett.*, 2018, **9**(23), 6814–6817.
28 X. Wang, K. Maeda, A. Thomas, K. Takanabe, G. Xin, J. M. Carlsson, K. Domen and M. Antonietti, *Nat. Mater.*, 2009, **8**, 76–80.
29 I. F. Silva, I. F. Teixeira, R. D. F. Rios, G. M. do Nascimento, I. Binatti, H. F. V. Victória, K. Krambrock, L. A. Cury, A. P. C. Teixeira and H. O. Stumpf, *J. Hazard. Mater.*, 2021, **401**, 123713.
30 G. Zhang, L. Lin, G. Li, Y. Zhang, A. Savateev, S. Zafeiratos, X. Wang and M. Antonietti, *Angew. Chem., Int. Ed.*, 2018, **57**, 9372–9376.
31 G. Zhang, G. Li, Z. A. Lan, L. Lin, A. Savateev, T. Heil, S. Zafeiratos, X. Wang and M. Antonietti, *Angew. Chem.*, 2017, **129**, 13630–13634.
32 Z. Chen, A. Savateev, S. Pronkin, V. Papaefthimiou, C. Wolff, M. G. Willinger, E. Willinger, D. Neher, M. Antonietti and D. Dontsova, *Adv. Mater.*, 2017, **29**, 1700555.
33 M. Y. Ye, S. Li, X. Zhao, N. V. Tarakina, C. Teutloff, W. Y. Chow, R. Bittl and A. Thomas, *Adv. Mater.*, 2020, **32**, 1903942.
34 B. Kurpil, K. Otte, A. Mishchenko, P. Lamagni, W. Lipiński, N. Lock, M. Antonietti and A. Savateev, *Nat. Commun.*, 2019, **10**, 1–10.
35 F. K. Kessler, Y. Zheng, D. Schwarz, C. Merschjann, W. Schnick, X. Wang and M. J. Bojdys, *Nat. Rev. Mater.*, 2017, **2**, 17030.
36 J. Yuan, Y. Tang, X. Yi, C. Liu, C. Li, Y. Zeng and S. Luo, *Appl. Catal. B Environ.*, 2019, **251**, 206–212.
37 V. W.-h. Lau, I. Moudrakovski, T. Botari, S. Weinberger, M. B. Mesch, V. Duppel, J. Senker, V. Blum and B. V. Lotsch, *Nat. Commun.*, 2016, **7**, 12165.